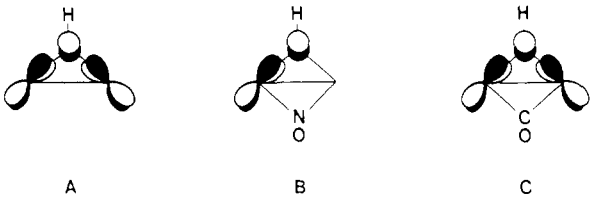

Figure 5. Lowest unoccupied molecular orbitals of (A) $[CpMn(CO)_2]_2(\mu\text{-}CH)^+$, (B) $[Cp_2Mn_2(CO)(NO)](\mu\text{-}NO)(\mu\text{-}CH)^+$, and (C) $[CpFe(CO)]_2(\mu\text{-}CO)(\mu\text{-}CH)^+$.

which for $[CpFe(CO)]_2(\mu\text{-}CO)(\mu\text{-}CH)^+$ is essentially an energetically isolated $p\pi$ orbital localized on the methylidyne carbon and oriented perpendicular to the Fe–CH–Fe plane. This orbital is easily accessible to nucleophiles. Looking once again at Figure 4, the interaction of the CH^+ $1\pi_y$ orbital with the $[CpFe(\mu\text{-}NO)]_2$ framework $8b_2$ orbital is strong enough that the antibonding counterpart (the orbital that is analogous to the LUMO of $[CpFe(CO)]_2(\mu\text{-}CO)(\mu\text{-}CH)^+$) is pushed above the Fe–Fe σ^* orbital. Therefore, the LUMO here is not a primarily CH^+-based orbital but rather is localized on the Fe atoms and directed along the metal–metal bond, thereby making this orbital sterically inaccessible and preventing facile nucleophilic addition.

The fact that $[CpFe(\mu\text{-}NO)]_2(\mu\text{-}CH)^+$ does not react with nucleophiles, and in particular alkenes, is disappointing since it was hoped the "hydrocarbation" reactions exhibited by $[CpFe(CO)]_2(\mu\text{-}CO)(\mu\text{-}CH)^+$[37] could be duplicated in a different system. This reaction is an important model of catalytic processes since it involves carbon–carbon bond formation between small organic fragments on a transition-metal dimer. Since we now understand what is required electronically for such reactivity, perhaps we can make use of this to predict what other bimetallic frameworks could form stable methylidyne-bridged complexes capable of exhibiting "hydrocarbation" reactivity. Calculations performed on two other (to our knowledge unknown) piano stool dimers indicate that they may provide the necessary electronic properties to induce such reactivity: $[CpMn(CO)_2]_2(\mu\text{-}CH)^+$ and $[Cp_2Mn_2(CO)(NO)](\mu\text{-}NO)(\mu\text{-}CH)^+$. The LUMO's calculated for each of these complexes are shown in Figure 5, along with the LUMO of $[CpFe(CO)]_2(\mu\text{-}CO)(\mu\text{-}CH)^+$. The similarity of the LUMO's of the two methylidyne-bridged manganese complexes with the iron dimer LUMO makes these compounds electronically well suited for similar reactivity with nucleophiles.

Acknowledgment. We gratefully acknowledge Dr. C. P. Casey, Dr. D. M. Roddick, Dr. W. A. G. Graham, and Dr. D. M. Heinekey for stimulating discussions and results prior to publication. R.H.C. is grateful for a Presidential Fellowship from The Ohio State University Graduate School.

(37) Casey, C. P.; Meszaros, M. W.; Fagan, P. J.; Bly, R. K.; Marder, S. R.; Austin, E. A. *J. Am. Chem. Soc.* **1986**, *108*, 4043–4053.

Magic Angle Spinning NMR Studies of Silicon Carbide: Polytypes, Impurities, and Highly Inefficient Spin–Lattice Relaxation

J. Stephen Hartman,* Mary F. Richardson,* Barbara L. Sherriff,† and Beatrice G. Winsborrow

Contribution from the Department of Chemistry, Brock University, St. Catharines, Ontario L2S 3A1, Canada. *Received November 28, 1986*

Abstract: Silicon carbide polytypes give distinctive ^{29}Si and ^{13}C MAS NMR spectra that can be related to the number and types of lattice sites present, which differ in their next-nearest-neighbor environment. It is shown that only four next-nearest-neighbor silicon (and carbon) environments are possible in crystalline silicon carbide regardless of polytype. A local-site designation system is developed for these and related to the various existing polytype designation systems. Carbon and silicon sites are isostructural, and the almost exact mirror-image relationship between ^{29}Si and ^{13}C chemical shifts of the 6H polytype indicates that the same structural factors determine chemical shifts of both nuclei. ^{13}C spin–lattice relaxation times can be extremely long and can differ considerably for nonequivalent lattice sites in the same sample, detracting from the reliability of ^{13}C MAS NMR as a tool for polytype studies. In the extreme case of cubic silicon carbide a ^{13}C signal has not yet been detected under a range of conditions that do give ^{29}Si spectra, consistent with ^{13}C spin diffusion being far less efficient than spin diffusion among the more abundant ^{29}Si atoms. Due to the long T_1's of atoms in crystalline silicon carbide sites, minor short T_1 impurities can be selectively detected by rapid pulsing, with little interference from signals of the bulk crystalline material. Hydrofluoric acid washing modifies the ^{29}Si short T_1 impurity signals to varying extents in different samples, indicating that they arise in part from surface oxide species.

The structure of silicon carbide is simultaneously very simple and very complex. All forms of silicon carbide are based on the diamond structure, with both silicon and carbon tetrahedral and with alternating silicon and carbon atoms. The basic structural types (polymorphs) are therefore hexagonal α–SiC (wurtzite structure) and cubic β–SiC (zinc blende structure). However, silicon carbide distinguishes itself from diamond in having many crystalline α–SiC modifications called polytypes.[1] These arise from the numerous possible stacking sequences of the silicon and carbon layers. The resulting unit cells have the same dimensions in two directions but differ in the third (the stacking direction.) A few short-period polytypes are stable under definite thermodynamic conditions; their transformations have been studied.[2] However, it is often observed that many different polytypes grow under the same conditions of temperature and pressure, several polytypes sometimes occurring side by side in the same crystal.[1]

† Present address: Department of Geology, McMaster University, Hamilton, Ontario L8S 4L8, Canada

(1) Verma, A. R.; Krishna, P. *Polymorphism and Polytypism in Crystals*; Wiley: New York, 1966.
(2) Jepps, N. W.; Page, T. F. In *Crystal Growth and Characterization of Polytype Structures*; Krishna, P., Ed.; Pergamon; Oxford, 1983; pp 259–307.

0002-7863/87/1509-6059$01.50/0

Crystal growth at screw dislocations is believed to give rise to polytypism in silicon carbide.[3] Approximately 200 polytypes of silicon carbide have been reported, and crystal structures of many have been determined.[4]

In addition to the inherent interest in its many polytypes, silicon carbide is an important industrial material. In the past its greatest importance has been in the abrasives industry,[5] and at present, through the development of innovative synthesis methods[6] and methods of compaction,[7] it is one of the most promising materials in the rapidly developing field of high-temperature ceramics.[8] Its synthesis and properties have been thoroughly studied[4,9] but much remains to be learned. Cubic silicon carbide has enormous potential as a semiconductor, but only recently has a method of crystal growth suitable for semiconductor applications been developed.[10]

High-resolution solid-state nuclear magnetic resonance spectroscopy utilizing the technique of magic angle spinning (MAS NMR) has become an enormously fruitful technique for structure determination in a wide range of inorganic materials,[11-13] notably in synthetic zeolites[14,15] and also in natural aluminosilicate minerals.[13,16] The technique has recently become important in the study of glasses and ceramics[17] where its sensitivity to local ordering i.e., to the number and types of atoms around a particular nucleus, provides information in situations where X-ray diffraction, with its requirement of long-range ordering, is less useful. MAS NMR is also being applied to silicon nitride and oxynitride[18] and to Si-Al-O-N phases.[19,20]

Silicon carbide is ideal for MAS NMR study since it consists of two elements, both having magnetically dilute spin $^1/_2$ isotopes (^{29}Si, 4.7%; ^{13}C, 1.1%). Unlike the oxygen-rich silicate minerals, no other elements are present to further dilute the NMR-active nuclei, so that both silicon and carbon atoms are present in silicon carbide at 80 M concentration. The resulting concentrations of ^{29}Si (3.8 M) and ^{13}C (0.88 M) are sufficient to allow good spectra to be obtained from a single scan on a high-field NMR instrument.

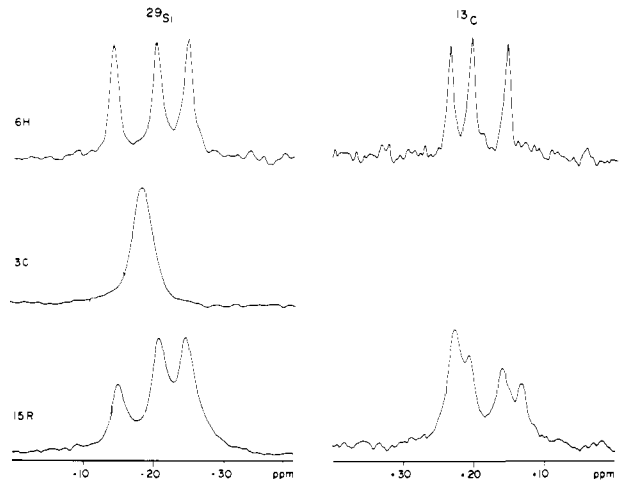

Figure 1. ^{29}Si and ^{13}C MAS NMR spectra of silicon carbide polytypes. Spectra were obtained at a magnetic field of 9.4 T with relaxation delays between pulses of at least 15 min.

Table I. Chemical Shifts of Silicon Carbide Polytypes[a]

	site type	6H	3C	15R
^{29}Si	A	-13.9	-18.3	-14.9
	B or C	-20.2		-20.8
	B or C	-24.5		-24.4
^{13}C				+13.3
	A[b]	+15.2	c	+16.0
	B or C[b]	+20.2		+20.7
	B or C[b]	+23.2		+22.7

[a] ppm to low field of tetramethylsilane. [b] Tentative assignment. [c] Not detected under a wide range of acquisition conditions.

However, as with other network solids such as diamond[21] and elemental silicon,[22] no efficient mechanism exists for spin-lattice relaxation, and long spin-lattice relaxation times can be a problem. This also represents an opportunity as short T_1 impurities can be selectively studied by NMR with negligible interference from the bulk silicon carbide.

We report here our NMR studies of silicon carbide polytypes and of minor components present in industrial silicon carbide samples. A preliminary communication of part of this work has appeared.[23] NMR without magic angle spinning has previously been used to investigate polymorphism and polytypism in silver iodide.[24] Structural polymorphism in molecular solids can be revealed by changes in MAS NMR chemical shift,[25] and chemical shift nonequivalences can be observed for chemically equivalent sites in molecules occupying nonequivalent sites in the crystal.[12] Our work represents the first application of MAS NMR to the study of polytypism.

Experimental Section

High-quality 6H and 3C silicon carbide crystals were obtained from the personal collection of the late Dr. G. R. Finlay. Further silicon carbide samples were obtained from General Abrasive division of Dresser Industries, Niagara Falls, Ontario. These included samples from batch production runs in which coke and silica sand are converted to silicon carbide through passage of an electric current.[5] Amorphous silicon carbide was provided by Dr. C. Schilling of Union Carbide Corp. and Nicalon ceramic fiber (primarily microcrystalline β-SiC; Nippon Carbon Co.) by Dr. P. E. D. Morgan of Rockwell International. The Nicalon fiber was degreased by washing with CH_2Cl_2 before spectra were obtained.

Single crystals of the 6H, 3C, and 15R polytypes were identified by their distinctive X-ray powder patterns.[26] The amorphous samples give

(3) Frank, F. C. *Philos. Mag.* **1951**, *42*, 1014. Mitchell, R. S. *Z. Krist.* **1957**, *109*, 1. Krishna, P.; Verma, A. R. *Z. Krist.* **1965**, *121*, 36. Pandey, D.; Krishna, P. *Philos. Mag.* **1975**, *31*, 1133.
(4) *Gmelin Handbook of Inorganic Chemistry*, 8th Ed.; Schlichting, J., Czack, G., Koch-Bienemann, E., Kuhn, P., Schroder, F., volume authors; Springer-Verlag: Berlin/Heidelberg/New York, 1984; Supplement Volume B2, Si-Silicon, "Properties of Crystalline Silicon Carbide".
(5) *Kirk-Othmer Encyclopedia of Chemical Technology*; 3rd ed.; Wiley: New York, 1978; Vol. 4, pp 520-535.
(6) Wynne, K. J.; Rice, R. W. *Annu. Rev. Mater. Sci.* **1984**, *14*, 297.
(7) Akashi, T.; Lotrich, V.; Sawaoka, A.; Beauchamp, E. K. *J. Am. Ceram. Soc.* **1985**, *68*, C-322.
(8) Sanders, H. J. *Chem. Eng. News* **1984**, *62*, (July 9), 26.
(9) *Gmelin Handbook of Inorganic Chemistry*, 8th ed.; Haase, V., Kirschstein, G., List, H., Ruprecht, S., Sangster, R., Schroder, F., Topper, W., Vanecek, H., Heit, W., Schlichting, J. volume authors; Springer-Verlag: Berlin/Heidelberg/New York, 1986; Supplement Volume B3, Si-Silicon, "System Si-C".
(10) Parsons, J. D.; Bunshah, R. F.; Stafsudd, O. M. *Solid State Technol.* **1985**, *28*, 133-139.
(11) Lippmaa, E.; Magi, M.; Samoson, A.; Tarmak, M.; Engelhardt, G. *J. Am. Chem. Soc.* **1980**, *102*, 4889.
(12) Fyfe, C. A. *Solid State N. M. R. for Chemists*; CFC: Guelph, Ontario, Canada, 1983.
(13) Oldfield, E.; Kirkpatrick, R. J. *Science (Washington, D.C.)* **1985**, *227*, 1537.
(14) Fyfe, C. A.; Thomas, J. M.; Klinowski, J.; Gobbi, G. C. *Angew. Chem., Int. Ed. Engl.* **1983**, *22*, 259.
(15) Thomas, J. M.; Klinowski, J. *Adv. Catal.* **1985**, *33*, 199.
(16) (a) Sherriff, B. L.; Hartman, J. S. *Can. Mineral.* **1985**, *23*, 205. (b) Sherriff, B. L.; Grundy, H. D.; Hartman, J. S. Presented at the International Mineralogical Association Conference, Stanford, CA, July 1986; Program Abstracts *14*, p 229. Sherriff, B. L.; Grundy, H. D.; Hartman, J. S. *Can. Mineral.*, in press.
(17) Engelhardt, G.; Nofz, M.; Forkel, K.; Wilsmann, F. G.; Magi, M.; Samoson, A.; Lippmaa, E. *Phys. Chem. Glasses* **1985**, *26*, 157. Dupree, R.; Holland, D.; Williams, D. S. *J. Non-Cryst. Solids* **1986**, *81*, 185. Gerstein, C.; Nicol, A. T. *J. Non-Cryst. Solids* **1985**, *75*, 423. Weeding, T. L.; de Jong, B. H. W. S.; Veeman, W. S.; Aitken, B. G. *Nature (London)* **1985**, *318*, 352.
(18) Dupree, R.; Lewis, M. H.; Leng-Ward, G.; Williams, D. S. *J. Mater. Sci. Lett.* **1985**, *4*, 393.
(19) Butler, N. D.; Dupree, R.; Lewis, M. H. *J. Mater. Sci. Lett.* **1984**, *3*, 469.
(20) Klinowski, J.; Thomas, J. M.; Thompson, D. P.; Korgul, P.; Jack, K. H.; Fyfe, C. A.; Gobbi, G. C. *Polyhedron* **1984**, *3*, 1267.
(21) Henrichs, P. M.; Cofield, M. T.; Young, R. H.; Hewitt, J. M. *J. Magn. Reson.* **1984**, *58*, 85 and references therein.
(22) Shulman, R. G.; Wyluda, B. J. *Phys. Rev.* **1956**, *103*, 1127.
(23) Finlay, G. R.; Hartman, J. S.; Richardson, M. F.; Williams, B. L. *J. Chem. Soc., Chem. Commun.* **1985**, 159.
(24) Brinkmann, D.; Freudenreich, W. *Z. Krist.* **1976**, *143*, 67.
(25) Lockhart, T. P.; Manders, R. F. *Inorg. Chem.* **1986**, *25*, 583. Also see ref 12, p 286.

the expected very diffuse powder patterns. Samples for NMR were ground in a tungsten carbide shatterbox and washed with dilute hydrochloric acid to remove traces of iron, a constant contaminant in crushed samples. Hydrofluoric acid washing experiments were carried out on HCl-washed material, using either 3% or 48% aqueous HF containing a trace of nitric acid, in a Teflon flask equipped with a Teflon-coated stirring bar.

Most NMR spectra were obtained on a Bruker WH-400 multinuclear Fourier Transform NMR spectrometer equipped with a 9.4-T superconducting magnet, using a home-built magic angle spinning probe,[27] with Delrin, Kel-F, or boron nitride rotors. ^{29}Si spectra were obtained at a frequency of 79.46 MHz by using 30° (3.7 μs) pulses, typically with 8K data points and a spectral width of 25 000 or 50 000 Hz, and Fourier transformed with 50 Hz of line broadening. ^{13}C spectra were obtained similarly, at a frequency of 100.58 MHz. A long recycle delay (minutes or hours) was frequently applied between scans to deal with long spin–lattice relaxation times. The samples were spun at approximately 3300 Hz at an angle of 54.7° to the magnetic field. Chemical shifts of sharp peaks are reproducible to ±0.1 ppm; both ^{29}Si and ^{13}C chemical shifts are reported in ppm to low field of tetramethylsilane. Spectra typically have spinning sidebands of moderate intensity (up to 20% of the total peak area); however, many spectra obtained under rapid-pulsing conditions (recycle delay of 0.1 s) did not give detectable spinning sidebands.

In favorable cases the spectrometer time required by long T_1 silicon carbide samples could be minimized by retuning the MAS probe[27] between ^{29}Si and ^{13}C while the probe and sample were still in the magnetic field. Over a period of hours while ^{29}Si spectra were being obtained, the ^{13}C magnetization was gradually approaching its equilibrium value, and retuning the probe to the ^{13}C frequency then allowed a ^{13}C spectrum to be obtained on the same sample with a single 90° pulse, without any additional relaxation delay.

^{13}C MAS NMR spectra were also obtained on a number of other Bruker NMR instruments (AC-200, CXP-200, and AM-500) under similar conditions, the principal aim being to obtain ^{13}C spectra of the 3C polytype. Particularly good resolution of 6H-polytype ^{13}C peaks was obtained on a probe manufactured by Doty Instruments, operating in a CXP-200 spectrometer and using alumina rotors, but a ^{13}C spectrum of the 3C polytype could not be obtained under any conditions so far attempted.

Results

MAS NMR spectra of the 6H, 3C, and 15R polytypes of silicon carbide are shown in Figure 1. Chemical shifts are given in Table I. The 6H polytype gives three well-resolved ^{29}Si peaks of equal intensity, corresponding to three equally populated silicon sites. Its ^{13}C spectrum also consists of three equal-intensity peaks, consistent with three equally populated carbon sites. The almost exact mirror-image relationship between the ^{29}Si and ^{13}C spectra extends even to the numerical values of chemical shifts in parts per million from tetramethylsilane (Table I). Resolution is dependent on the relaxation delay between pulses, with longer delays giving better resolution.

The 15R polytype has ^{29}Si and ^{13}C chemical shifts very similar to those of the 6H polytype (Table I), consistent with the same three types of silicon and carbon site being present in each. The peaks are less well-resolved, consistent with lower purity of this sample which was a typical crystal from an industrial production run. ^{29}Si peak intensities are in the ratio 1:2:2. The ^{13}C spectrum is less readily obtained and less straightforward. Relative peak intensities are different, and a fourth peak is present. All peaks but the +13.3 ppm peak correspond closely in chemical shift to ^{13}C peaks of the 6H polytype. Similar relative ^{13}C peak intensities are obtained with either a 15-min or a 1 h relaxation delay between 30° pulses.

The 3C polytype gives a single ^{29}Si peak, consistent with all silicon atoms being crystallographically equivalent. We have not yet been successful in detecting a ^{13}C signal from cubic silicon carbide despite a number of attempts, including (i) multiple 30° pulse accumulations at 9.4 T extending over at least 12 h with 5-, 300-, and 900-s delays between pulses, (ii) single 90° pulse experiments at 4.7, 9.4, and 11.7 T, following an overnight relaxation delay of at least 12 h, and (iii) a single 90° pulse experiment at 4.7 T, following a relaxation delay of 62 h. An extremely long spin–lattice relaxation time is indicated.

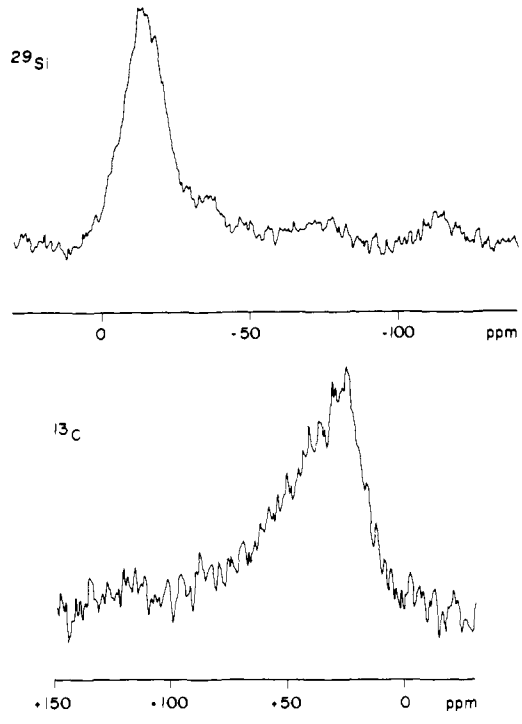

Figure 2. MAS NMR spectra of Nicalon ceramic fiber (5-s relaxation delay between pulses): ^{29}Si, 654 scans, 9.4 T, Delrin rotor; ^{13}C: 300 scans, 4.7 T, alumina rotor.

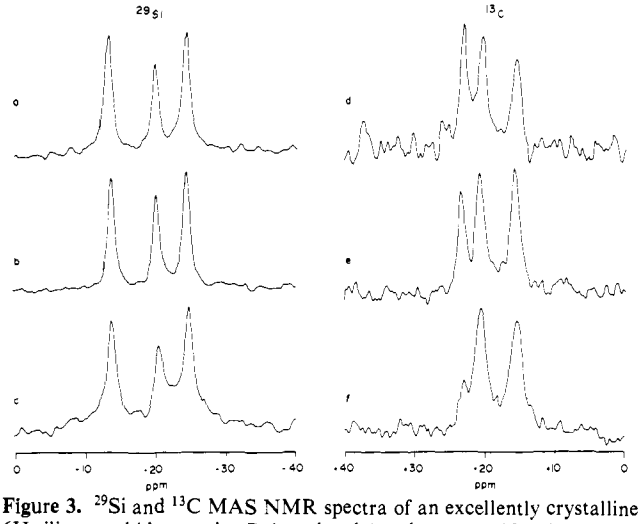

Figure 3. ^{29}Si and ^{13}C MAS NMR spectra of an excellently crystalline 6H silicon carbide sample. Relaxation delays between 30° pulses are as follows: a and d, 15 min; b and e, 5 min; c and f, 5 sec.

Amorphous silicon carbide gives broad and featureless ^{29}Si and ^{13}C signals (Figure 2). Chemical shifts for Nicalon ceramic fiber are as follows: ^{29}Si, −14.5 ppm, and ^{13}C, +25 ppm. Approximate peak widths at half-height are 18 ppm (^{29}Si, 9.4 T) and 16 ppm (^{13}C, 4.7 T). While the ^{29}Si peak width is little affected by rapid vs. slow pulsing, the ^{13}C peak is broadened considerably (to a peak width at half-height of 58 ppm) when 30° pulses are applied every 0.1 s rather than every 5 s. The ^{29}Si spectrum contains minor peaks at −75 ppm (elemental silicon absorbs at −80.6 ppm) and at −112 ppm (consistent with SiO_2). A sample of amorphous silicon carbide provided by Union Carbide Corp. gave slightly narrower peaks with similar chemical shifts (^{29}Si, −15.9 ppm; ^{13}C, +19 ppm) and negligible additional ^{29}Si peaks.

Figure 3 shows variations in ^{29}Si and ^{13}C relative peak intensities with relaxation delay between 30° pulses, in spectra of a sample of predominantly 6H silicon carbide. The variations are especially pronounced in the ^{13}C spectra, with one of the ^{13}C peaks almost

(26) Thibault, N. W. *Am. Mineral.* **1944**, *29*, 327.
(27) Fyfe, C. A.; Gobbi, G. C.; Hartman, J. S.; Lenkinski, R. E.; O'Brien, J. H.; Beange, E. R.; Smith, M. A. R. *J. Magn. Reson.* **1982**, *47*, 168.

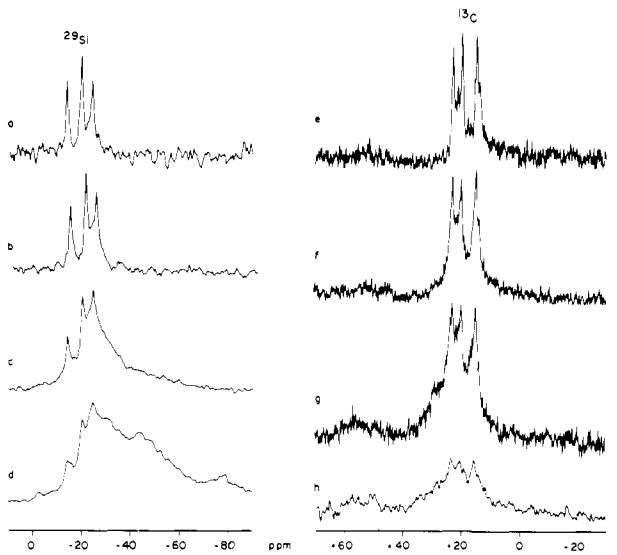

Figure 4. Effects of variation in relaxation delay on ^{29}Si and ^{13}C MAS NMR spectra of a commercial sample of silicon carbide abrasive powder. Relaxation delays between 30° pulses are as follows: a and e, 15 min; b and f, 30 sec; c and g, 5 sec; d and h, 0.5 sec.

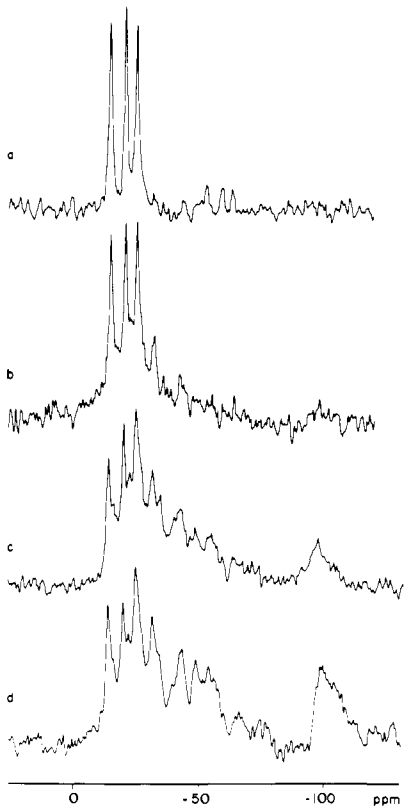

Figure 5. ^{29}Si MAS NMR spectra of a crystal of industrial abrasive grade 6H silicon carbide (General Abrasive, Niagara Falls, Ontario). Relaxation delays between 30° pulses are as follows: a, 5 min; b, 1 sec; c, 0.5 sec; d, 0.1 sec.

vanishing when pulses are separated by only a 5-s relaxation delay, consistent with unequal spin–lattice relaxation times for the different sites.

Figures 4 and 5 show that NMR peaks due to minor short T_1 impurity species in dark gray industrial abrasive-grade silicon carbide appear as a disproportionate share of the total signal when rapid pulsing is carried out to saturate the long T_1 nuclei in the bulk crystalline material. The appearance of the ^{29}Si spectrum is totally changed. Pale green or colorless samples of 6H silicon carbide, known to be of higher purity, do not give detectable impurity peaks under similar acquisition conditions. The short

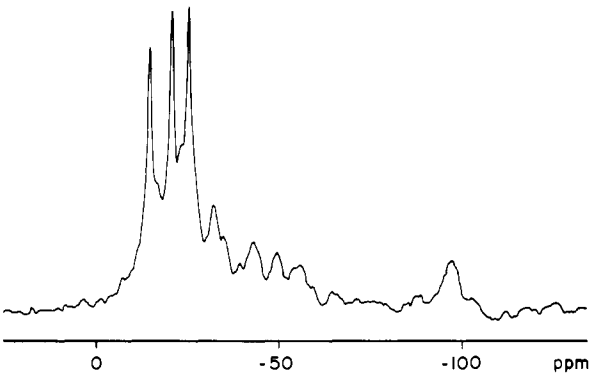

Figure 6. ^{29}Si MAS NMR spectrum of a different crystal of abrasive grade 6H silicon carbide, obtained with a relaxation delay between 30° pulses of 0.1 s. Components seen in Figure 5D are present in different proportions.

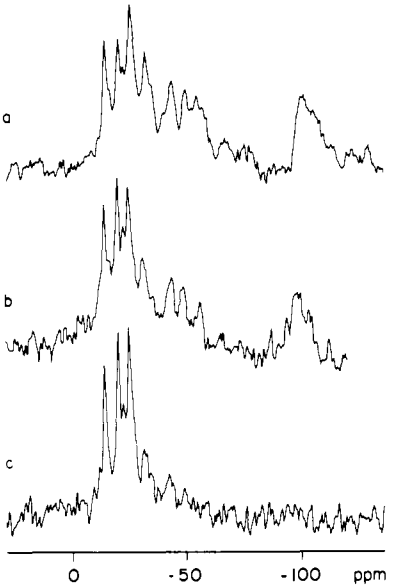

Figure 7. Rapid-pulsing ^{29}Si MAS NMR spectra of industrial abrasive grade 6H silicon carbide (same crystal as Figure 5; 0.1-s recycle delay), showing the effects of washing with 3% aqueous hydrofluoric acid: a no HF washing; b, 1-h wash; c, 65-h wash.

T_1 species make up no more than a few percent of the total silicon and, not surprisingly, vary considerably among different samples. However some ^{29}Si peaks recur in many samples: −32.4, −44, −49, −56, and −97 ppm (Figure 6) and sometimes −79 ppm.

Similar changes are apparent in the ^{13}C spectra (Figure 5), with broadening of the signals and appearance of a broad resonance to low field of the crystalline SiC peaks. However in our work the rapid-pulsing ^{13}C spectra have been partially obscured by the rotor ^{13}C resonances (Delrin or Kel-F), which occur well to low field of the crystalline SiC resonances.

Figure 7 shows the disappearance of much of the short T_1 impurity peak intensity on washing an industrial 6H-polytype sample with 3% HF. An underlying broad resonance band survives. However many industrial samples do not respond to HF treatment to this extent; some show only a sharpening of some of the minor-component resonances. Preliminary ^{19}F MAS NMR attempts to detect surface fluorine incorporated by HF washing have not been successful, although ESCA analysis does show the presence of fluorine at the surface.

Discussion

I. Site Geometries in Silicon Carbide Polytypes. Since NMR is a probe of the local site environment, a local-site designation system is desirable and is here developed and related to the various existing lattice designation systems for polytypes.

A. Polytype Structures and Notations. Silicon carbide is readily visualized as a layer structure in spite of its three-dimensional

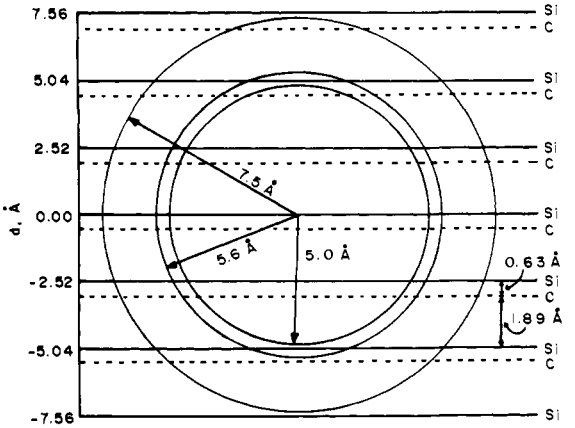

Figure 8. Layers surrounding an arbitrary central layer of silicon atoms. The 5-Å sphere does not quite reach the silicon layers at ±5.04 Å. The 5.6-Å sphere stops short of the carbon layer at ±5.67 Å, and the 7.5-Å sphere stops short of the silicon layers at ±7.56 Å.

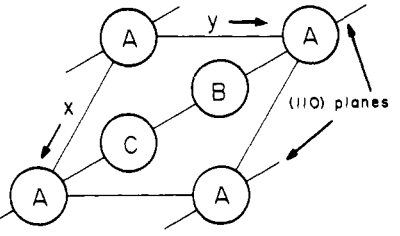

Figure 9. The hexagonal unit cell showing the A, B, and C positions at (0, 0), ($^1/_3$, $^2/_3$), and ($^2/_3$, $^1/_3$), respectively. Atoms in the A, B, and C positions lie on the (110) planes.

nature. Hexagonal close-packed layers of silicon atoms stack on each other in such a way that each atom in the upper layer fits in a valley formed by the junction of three silicon atoms in the layer below, and vice versa. The carbon atoms occupy half of the tetrahedral holes thus formed. Adjacent silicon layers are ca. 2.52 Å apart, and there is a carbon layer ca. 1.89 Å above each silicon layer (Figure 8).[1] Very accurate structural work[28] has revealed slight differences in the Si–Si (and C–C) layer spacings in the 6H polytype, and these presumably exist in other polytypes too, but this is not crucial for the subsequent discussion.

Several notations exist for describing different polytypes.[1] The Ramsdell notation consists of a two-part symbol, the first part being the number of layers in the unit cell and the second part a letter (C, H, R) designating the lattice type (cubic, hexagonal, and rhombohedral). The common SiC polytypes are 2H, 3C, 6H, and 15R.[1,2] The 3C form is the only cubic one and is also referred to as β-SiC; the remaining polytypes are collectively called α-SiC.

The ABC notation is convenient for describing the actual positions of the atoms in a close-packed structure.[29] In the initial silicon layer, the atoms lie on the edges of the unit cell with x and y coordinates (0, 0) and translationally equivalent positions at (1, 0), (0, 1), and so on, as shown in Figure 9. Atoms with these coordinates form the A layer. The atoms in the next silicon layer occupy one of two sets of valleys: the ones at ($^1/_3$, $^2/_3$) or the ones at ($^2/_3$, $^1/_3$). These coordinates describe the B and C positions, respectively. The cubic form of SiC has .../ABC/ABC... stacking, 6H has .../ABCACB/... stacking, and so on,[1] where slashes designate unit cell boundaries. If the positions of the carbon atoms are included as lower case letters, these sequences become / AaBbCc/ and /AaBbCcAaCcBb/, respectively.

Although the ABC notation gives a complete description of the structure, it is cumbersome and alternative descriptions have been devised.[1] The Zhdanov sequences are especially convenient for our subsequent discussion of types of silicon (or carbon) environments in different polytypes. Ramsdell noted that all atoms

(28) Gomes de Mesquita, A. H. *Acta Crystallogr.* **1967**, *23*, 610.
(29) Wells, A. F. *Structural Inorganic Chemistry*, 5th Ed.; Clarendon: Oxford, 1984; pp 145–158.

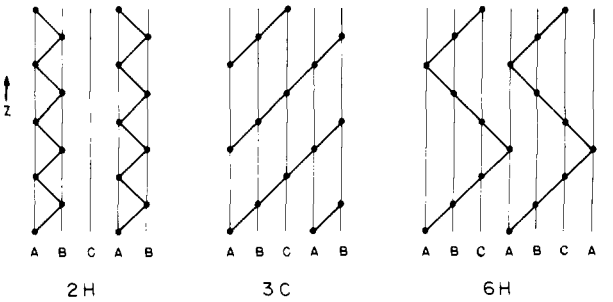

Figure 10. Ramsdell zigzag diagrams for some simple SiC polytypes. The 2H polytype has an /AB/AB... stacking of silicon atoms, corresponding to a Zhdanov symbol of (11). The 3C and 6H polytypes have silicon stacking sequences of /ABC/ABC... and /ABCACB/..., respectively corresponding to Zhdanov symbols of (∞) and (33). Carbon atoms have been omitted for simplicity.

in silicon carbide polytypes lie on the (110) planes (Figure 9) and that on these planes the atoms lie in zigzag patterns characteristic of the stacking, as can be seen for the 2H, 3C, and 6H polytypes (Figure 10). In the 6H form, the sequence moves three positions to the right (a "zig" of A → B → C → A) before reversing and moving three positions back to the left (a "zag" of A → C → B → A). This corresponds to the Zhdanov symbol (33), i.e., three shifts to the right followed by three to the left. Similarly the 2H and 3C polytypes have Zhdanov symbols (11) and (∞), respectively.

B. Differences in the Surroundings of Silicon and Carbon in Different Polytypes. We first examine the magnitude of variation in the SiC_4 primary coordination tetrahedron, as the immediate neighbors of an atom are expected to contribute most to the chemical shift. Fortunately the 6H polytype has been the subject of a very careful X-ray structure determination.[28] The three crystallographically independent Si atoms have identical nearest-neighbor surroundings within experimental error: each Si has one long Si–C bond along the stacking axis and three shorter Si-C bonds of equal length. These distances are 1.894 and 1.886 Å for Si(1), 1.891 and 1.886 Å for Si(2), and 1.894 and 1.885 Å for Si(3), all ±0.002 Å. All C–Si–C angles lie between 109.4 and 109.5°. Such small variations in the primary coordination sphere, beyond the accuracy limits of the most careful X-ray structural work, are unlikely to have much effect on the chemical shift. We thus consider variations in additional shells of neighbors, initially out to a distance of 5.0 Å.

Consider a silicon atom, arbitrarily defined to be in an "A" layer. Out to 5.0 Å, there are two layers of carbon atoms and a layer of silicon atoms on either side (the inner circle in Figure 8). The stacking sequences of these layers define four unique types of surroundings of a silicon atom, which can be shown as follows. The central A layer of silicons can have either a B or a C (but not an A) layer on either side. However, the sequence BbAaBb is equivalent to CcAaCc after a 60° rotation, and similarly BbAaCc is equivalent to CcAaBb. Taking CcAaBb and BbAaBb as the unique sequences, we add a carbon layer below the central layer to complete the surroundings out to 5 Å. Thus, the four types of Si are bCcAaBb, cBbAaBb, aCcAaBb, and aBbAaBb, which we designate types A, B, C, and D, respectively. The type A sequence bCcAaBb is identical with the sequences cAaBbCc, aBbCcAa, cBbAaCc, aCcBbAa, and bAaCcBb; similar equivalences hold for the other types.

Table II lists the surroundings of a central silicon atom out to 5 Å for each of the four types, and Figure 11 shows SiC_4 tetrahedra embedded in the shell of second neighbors. The geometries of these shells are significantly different: in type A, the 12 silicon second neighbors are located at the corners of a cuboctahedron, whereas in Type B, they are located at the corners of a twinned cuboctahedron (3:6:3 structure). Types C and D are characterized by having 13 second neighbors, 12 silicons and a carbon; in these, the carbon atom caps a trigonal face of the types A and B polyhedra to give respectively a capped cuboctahedron and a capped twinned cuboctahedron.

Table II. Silicon Surroundings in Silicon Carbide Polytypes Out to 5 Å

type	neighbors	geometry	dist to central Si, Å
A	4 C	tetrahedron	1.89
	12 Si	cuboctahedron	3.08
	12 C	no established name	3.61
	6 Si	octahedron	4.36
	12 C	no established name	4.75
B	4 C	tetrahedron	1.89
	12 Si	twinned cuboctahedron	3.08
	12 C	no established name	3.61
	6 Si	trigonal prism	4.36
	12 C	no established name	4.75
C	4 C	tetrahedron	1.89
	12 Si, 1 C	capped cuboctahedron	3.08, 3.15
	9 C	no established name	3.61
	6 Si, 6 C	no established name	4.36, 4.40
	9 C	no established name	4.75
D	4 C	tetrahedron	1.89
	12 Si, 1 C	capped twinned cuboctahedron	3.08, 3.15
	9 C	no established name	3.61
	6 Si, 6 C	no established name	4.36, 4.40
	9 C	no established name	4.75

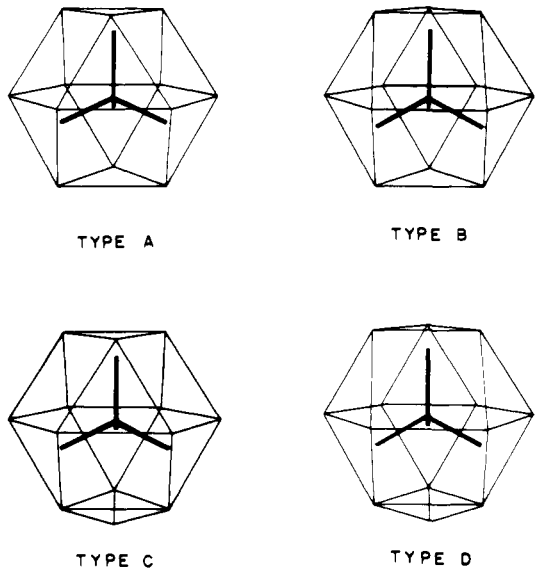

Figure 11. First and second neighbors for the four possible types of silicon (and carbon) surroundings in silicon carbide polytypes.

C. Determination of the Relative Numbers of Type A–D Atoms in a Polytype. The simplest method of determining how many silicon atoms of each type can be found in a particular polytype is to convert the ABC sequences for the A–D sites to their Ramsdell zigzags and the corresponding Zhdanov numbers. The Zhdanov symbols for the polytypes then directly yield the number of silicon atoms of each type. Figure 12 shows that the type A sequence bCcAaBb can only be obtained if a Zhdanov number ≥3 occurs in the polytype symbol. Similarly types B, C, and D can only be found when the Zhdanov numbers are (≥2)(≥1), (≥1)(≥2), and (≥1)(1)(≥1), respectively. As an example, consider the 15R polytype whose Zhdanov symbol is .../323232/3..., where the slashes indicate unit cell boundaries. The number "3" occurs three times, thus showing that there are three type A silicons. The Zhdanov sequence (≥2)(≥1) is found in six sequences, /32, 23, 32, 23, 32, and 2/3, so there are six type B silicons. Similarly are found six type C silicons.

Table III summarizes the types and numbers of silicon (and carbon) atoms in several common polytypes and a few unusual ones. It is clear that, in general though not always, the polytypes differ in the relative number and types of silicon atoms. For example, the 4H polytype contains only types B and C silicons, whereas the 3C polytype has only type A and the 2H polytype has only type D. The 6H and 15R polytypes both contain types A, B, and C silicons, but the ratios of the types are different. The two 51R polytypes are significantly different, the most common form having types A, B, and C in the ratio 5:6:6 and the less common form having them in the ratio 1:8:8. However, there are instances in which different polytypes have the same ratio of A:B:C types, e.g., 15R and 45R. This is readily predictable since the Zhdanov symbols have the same proportions of 2's and 3's, and we are limiting ourselves to surroundings less than two layers away from the central layer.

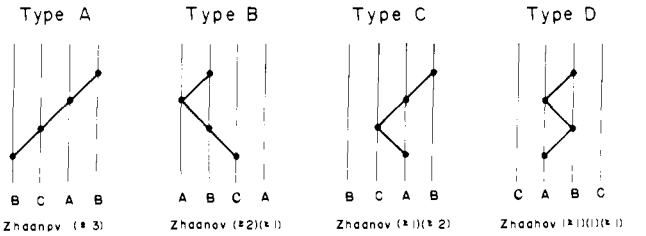

Figure 12. Zigzag sequences and corresponding Zhdanov symbols for the four types of silicon surroundings. Carbon atoms have been omitted for simplicity. The sequences shown are BC*A*B (type A), CB*A*B (type B), AC*A*B (type C), and AB*A*B (type D). The atom in italics is the central silicon.

Table III. Number and Types of Silicon (Carbon) Atoms in Different Polytypes of Silicon Carbide

polytype	Zhdanov symbol[a]	no. of Si (C) atoms with surroundings of type A	type B	type C	type D
2H	(11)				2
3C		3			
4H	(22)		2	2	
6H	(33)	2	2	2	
8H	(44)	4	2	2	
9R	$(21)_3$		3	3	3
15R	$(32)_3$	3	6	6	
21R	$(34)_3$	9	6	6	
33R	$(3332)_3$	9	12	12	
45R	$(232233)_3$	9	18	18	
51R[b]	$(333332)_3$	15	18	18	
51R[c]	$(22222223)_3$	3	24	24	

[a] All Zhdanov sequences from: Schaffer, P. T. B. *Acta Crystallogr., Sect. B: Struct. Crystallogr. Cryst. Chem.* **1969**, *B25*, 477 except for 45R from: Pandey, D.; Krishna, P. *Philos. Mag.* **1975**, *31*, 1133 and 9R from: Jepps, N. W.; Smith, D. J.; Page, T. F. *Acta Crystallogr., Sect. A: Cryst. Phys., Diffr., Theor. Gen. Crystallogr.* **1979**, *A35*, 916. [b] More common 51R polytype. [c] Less common 51R polytype.

A number of other features are also apparent from Table III and can be readily explained. Type D silicon is infrequent since the Zhdanov symbol must contain a "1"; this requirement is satisfied for only the 2H polytype and some rare polytypes such as 9R.[4] Further, the number of type B atoms is always equal to the number of type C atoms. This is due to the fact that any sequence of the type $(m)(n)(o)$ where $n \geq 2$ has to have a type C atom at one end (≥1)(≥2) and a type B atom at the other (≥2)(≥1). To put it more simply, when a "zig" of any length changes direction, the "zag" at the bottom gives a type C atom and the "zag" at the top gives a type B atom. Finally, polytypes with large numbers of "3's" or higher in their symbols will have relatively large numbers of type A silicon atoms in their structures, as can be seen by comparing 6H with 8H, or the two 51R polytypes.

In any silicon carbide polytype the carbon surroundings exactly mirror the silicon surroundings, provided only that the spacing between adjacent like atom layers remains constant. This condition appears to be met within a few thousandths of an angstrom. Thus the numbers and types of carbon atoms will be identical with the numbers and types of silicon atoms in all polytypes. Rarely are two elements of the same group of the periodic table in essentially identical crystallographic environments in the same compound, allowing factors affecting their chemical shifts to be compared so directly; thus silicon carbide chemical shifts can provide a test

of how closely chemical shifts reflect the geometry of the lattice site.

II. Polytype NMR Spectra. The three-peak ^{29}Si spectra of the 6H and 15R polytypes with their 1:1:1 and 1:2:2 relative intensities confirm our analysis of number and types of local site (Table III) and confirm the importance of non-nearest-neighbor geometry in determining chemical shift. From relative intensities of the 15R peaks and the similar ^{29}Si chemical shifts observed in both polytypes, the lowest field resonance (−13.9 ppm in 6H; −14.9 ppm in 15R) is readily assigned to type A silicon. However an empirical assignment of the peaks due to type B and type C silicons cannot be made on the basis of intensities since the numbers of type B and type C atoms are the same in any polytype.

Since a particular next-nearest-neighbor geometry always brings with it the same geometries in the next three layers (Table II), the next-nearest-neighbor effects on chemical shift, which probably predominate, cannot readily be disentangled from the effects of the more distant polyhedra out to 4.75 Å. However, types A and B have the same number of neighbors in each shell out to 4.75 Å, and these numbers differ from those in types C and D which also share the same number of neighbors in each shell. Hence types A and B chemical shifts are likely to be more similar to each other than to those of types C or D; on this tenuous basis the −20.8 ppm peak seems more likely to arise from type B than from type C.

If surroundings further than 5 Å from the central atom have a detectable effect on its chemical shift, distinction between type B and type C resonances is in principle possible. The 15R polytype has five crystallographically nonequivalent sites, of which two are type B and two are type C. The two kinds of type C site become different if an additional layer of silicon atoms on either side of the central layer is taken into account; i.e. differences in surroundings begin to occur at 5.02 Å (Figure 8). The two kinds of type B site retain identical neighbor geometries at 5.02 Å and only become different at ca. 6 Å if another layer of carbons is added. Thus if sufficiently high resolution could be attained, one would expect a greater broadening or splitting of the type C peak than of the type B peak. In other words, there should be three peaks in the ratio 2:2:1 if surroundings out to less than 5 Å determine the chemical shift, four peaks in the ratio 2:1:1:1 if surroundings out to 5.6 Å determine the shift, and five peaks in the ratio 1:1:1:1:1 if surrounding out to 7.5 Å determine the shift. In general, the four types of stacking described in section I and Table II become eight if surroundings to 5.6 Å are considered and 16 if surroundings to 7.5 Å are considered. However, these stackings are not all equally likely (many contain the Zhdanov symbol "1" in their sequence), so the number of NMR peaks is still relatively limited. Thus the more common 51R form, with 17 crystallographically independent silicons, should exhibit only five peaks in the ratio 5:5:1:5:1 even if surroundings out to 7.5 Å determine the shift.

^{29}Si peak widths are greater in our 15R spectra than in our 6H spectra, but this is not related to differences within type B, or type C, sites since the low-field peak, arising from the single type A site, is broad as well. Impurities apparently cause the broadening; the only 15R polytype samples available to us were industrial production-run samples.

Cubic silicon carbide (the 3C polytype) has only type A silicon, consistent with the single ^{29}Si peak observed, but its −18.3 ppm chemical shift is different from that of any of the 6H or 15R peaks. Symmetry differences in the nearest-neighbor shell probably account for the discrepancy. The silicons (and carbons) in the cubic form have full tetrahedral symmetry whereas in all other polytypes there must be one long and three short bonds, as a result of the c/a ratio being greater than ideal for close-packed spheres.[28]

The great similarities in ^{13}C chemical shift between the 6H and 15R polytypes (Table I) are a reasonable basis for empirically correlating corresponding ^{13}C peaks of the two polytypes, as with their ^{29}Si peaks. The 6H-polytype relative peak intensities are the expected 1:1:1. However the 15R-polytype ^{13}C spectrum (Figure 1) is anomalous, containing four peaks rather than the three peaks expected. Resolution is not good but relative peak intensities may be consistent with 2:1:1:1, which would correspond to the differences in neighbors beyond 5 Å. However such a major change in chemical shift with a change in distant neighbors seems unlikely. Identification of the extra peak at +13.3 ppm awaits further work, and we are now seeking additional 15R-polytype samples. The possibility of major carbon-containing impurities in our present best 15R-polytype sample cannot yet be discounted.

The mirror image relationship between ^{29}Si and ^{13}C spectra of the 6H polytype (Figure 1) is intriguing. The almost identical magnitude, but opposite sign, of the chemical shifts of the two nuclei arises from the use of tetramethylsilane as the reference compound for both nuclei. Tetramethylsilane is in essence a small fragment of the silicon carbide structure with outer silicons replaced by hydrogens. Hydrogen and sp^3 silicon have very similar electronegativities on the Mulliken–Jaffé scale, so the substitution should have little effect on the local diamagnetic shielding term. The silicon carbide ^{29}Si shifts do cover a slightly greater range than the ^{13}C shifts, consistent with a larger local paramagnetic shielding term for the heavier nucleus. However the changes in chemical shift from the TMS value, and more fundamentally the chemical shift differences among lattice sites, should be primarily due to neighbor anisotropy effects of the next-nearest-neighbor and further-out polyhedra. Since each carbon site is to a good approximation isostructural with a silicon site, ^{29}Si and ^{13}C neighbor anisotropy effects on chemical shift could well mirror each other.

Insufficient information in available to unambiguously assign the ^{13}C peaks, so the possibility remains that the apparent mirror-image relationship of ^{29}Si and ^{13}C chemical shifts is a coincidence. The type A peak, at lowest field in the ^{29}Si spectrum, should be identifiable from relative peak areas in the ^{13}C spectra of other polytypes such as 15R and should come at highest field if the mirror-image relationship is real. However, extremely inefficient ^{13}C spin–lattice relaxation, a serious problem in the 3C polytype and perhaps in other polytypes as well, may render ^{13}C data ambiguous. A more reliable verification of the mirror image chemical shift relationship should come from chemical shifts of the type D sites in the 2H or 9R polytypes. If the mirror image relationship holds we can predict chemical shifts of approximately −31 ppm (^{29}Si) and +28 ppm (^{13}C) for type D, by extrapolation of the second-neighbor geometrical relationships and chemical shifts of types A–C.

III. Consequences of Highly Inefficient Spin–Lattice Relaxation. There must be great variations in spin-lattice relaxation times among and within our silicon carbide samples. Our inability to detect a ^{13}C resonance of cubic (3C) silicon carbide, despite numerous attempts including very long periods of "soaking in the magnetic field" to allow equilibration of spin states before pulsing, is in striking contrast to the ease of obtaining ^{29}Si spectra from the same samples and indicates a vast difference between ^{29}Si and ^{13}C T_1's. Yet ^{13}C as well as ^{29}Si spectra are readily obtained from the 6H polytype. Our 15R sample appears to have ^{13}C T_1's intermediate between those of the 3C and 6H samples.

Unequal T_1's for the different ^{29}Si (and ^{13}C) sites are indicated by variations in relative peak intensities as the relaxation delay between pulses is changed (Figure 3). In our preliminary communication[23] we interpreted differences in ^{29}Si peak intensities in this sample as due to the presence of polytypes in addition to 6H, and consistent with this the X-ray powder pattern does show weak additional lines. However in section I above we have demonstrated that *any* polytype must have equal numbers of type B and C sites, so the unequal intensities of the −20.2 and −24.5 ppm peaks cannot arise from any possible mixture of polytypes. T_1 differences are the only plausible explanation. Note that one of the ^{13}C peaks almost vanishes when pulses are separated by a 5-s relaxation delay, vividly illustrating the hazards to spectra interpretation if there are unsuspected long T_1 components.

Extremely long spin–lattice relaxation times have been reported for a number of network solids such as diamond,[21] elemental silicon,[22] and quartz,[30] consistent with our observations on silicon

(30) Holzman, G. R.; Anderson, J. H.; Koth, W. *Phys. Rev.* **1955**, *98*, 542.

carbide, and affect NMR work in a number of ways. None of the relaxation mechanisms involving molecular tumbling that are effective in solution are applicable. Instead, spin–lattice relaxation is expected to be dominated by traces of paramagnetic impurities, which can vary from sample to sample, and by spin diffusion from the paramagnetic sites.[31] Spin diffusion is a mutual spin flip process, in which like nuclei that are coupled by the dipolar interaction exchange spin states. Since the dipolar interaction drops off very sharply with distance, the probability of a mutual spin flip is much greater for more abundant nuclei, consistent with ^{29}Si spin–lattice relaxation being more efficient than ^{13}C spin–lattice relaxation in silicon carbide. Others have concluded that spin diffusion is unlikely to be efficient with nuclei as magnetically dilute as ^{13}C.[21,32] Since the ^{13}C concentration is lower in silicon carbide than in diamond, an enormously long ^{13}C spin–lattice relaxation time for cubic silicon carbide (isostructural with diamond) is not surprising.

Uniformly distributed paramagnetic impurities can enhance the collection of NMR signals by acting as "relaxation reagents".[33] However, if the traces of paramagnetic impurities that dominate spin–lattice relaxation in solids are not uniformly distributed and if spin diffusion is not efficient, signals from impurity-rich regions can be selectively enhanced. This is the case in some of our silicon carbide samples since spectral resolution can be improved, with no change in relative peak areas, by increasing the relaxation delay between pulses. In such cases more rapid pulsing apparently favors signals from short T_1 atoms in lattice sites near paramagnetic centres, which broaden the signals of nearby atoms but have little effect on chemical shift. Our work on feldspar minerals has shown similar effects: increasing iron content leads first to greater ease of obtaining ^{29}Si spectra due to more efficient spin–lattice relaxation, until excessive line broadening interferes.[16a] However quartz, clearly visible in thin sections of the same feldspar samples, was not detected in the ^{29}Si spectra, consistent with a very early report of a 10-h ^{29}Si T_1 for quartz[30] and with the expected partitioning of traces of iron into feldspar rather than quartz when the separate mineral phases crystallize. Thus whenever more than one type of local region is present, even in a single-phase system if paramagnetic impurities do not affect all nuclei to the same extent, it is difficult to determine whether the NMR spectrum is representative of the sample as a whole. Such problems are particularly acute in coals and polymers and have been investigated in detail in these systems.[34] Underrepresentation of carbon magnetization in ^{13}C spectra of coals appears to be general,[34,35] and a similar situation may apply in silicon carbide.

A further factor is the semiconductor nature of silicon carbide, which is readily doped to give both p- and n-type material. Bloembergen, in an early analysis of relaxation in semiconductors,[36] concluded that in elemental silicon ^{29}Si spin–lattice relaxation should be accomplished by an interaction between the nuclear spins and the spins of the mobile electrons or holes, and indeed T_1 in elemental silicon is very strongly dependent on mobile electron or hole concentrations, approaching a limit of several hours as these concentrations diminish.[22] Early low-temperature work on doped silicon carbide using electron nuclear double resonance did show T_1 variations with dopant concentrations,[37] and suitably doped samples of the 3C polytype should readily give ^{13}C MAS spectra.

IV. Selective Detection of Short T_1 Impurities. The appearance of short T_1 impurity peaks as a disproportionate share of the total signal under rapid pulsing conditions (Figures 4 and 5) provides a means of studying very minor silicon carbide impurities by NMR. This is analogous to the use of ^{29}Si CP/MAS NMR to selectively emphasize the surface silicons of silica gel, since only these are close enough to the surface OH groups to be effectively cross-polarized.[38] The three peaks of crystalline 6H silicon carbide become swamped by signals due to minor but fast-relaxing components which are not representative of the sample as a whole. Note that a 5-s delay between 30° pulses, commonly used in ^{29}Si MAS NMR, can give a highly distorted picture of the sample. The recurrence of the same short T_1 ^{29}Si peaks in 6H polytype samples from a range of sources shows that the same impurities are present and indicates that rapid-pulsing ^{29}Si NMR will be a valuable tool for the study of common silicon carbide impurities. Spectra do show significant variations from sample to sample (compare Figures 4d, 5d, and 6), not surprisingly since preparation conditions vary, and higher purity crystals do not give detectable impurity peaks under the same conditions.

Silicon carbide impurities are quite varied, and some have been extensively studied.[4,9] We can tentatively suggest some impurity peak assignments, based on the fact that oxygen is a common contaminant of industrial silicon carbide. Oxide contamination, sometimes formulated as $Si_xC_yO_z$ indicating intimate association of the oxygen with the SiC lattice, is a well-known problem in the compaction of silicon carbide powders.[7] Oxidation to SiO_2 can occur at high temperatures, and SiO_2 can occur as a film on silicon carbide crystal surfaces. Amorphous silicon carbide can contain considerable SiO_2 and carbon as well as its principal component of microcrystalline β-SiC.

The −97 ppm peak is consistent with some silicates but not with SiO_2 which has a chemical shift range of −108.1 to −119.4 ppm in its various four-coordinate forms.[39] (Heating of finely ground 3C silicon carbide at 1100 °C does give a broad peak at −110 ppm, consistent with its known oxidation to SiO_2 under these conditions.) The −97 ppm peak might, instead, correspond to tetrahedral silicon bonded to three oxygens and one carbon; such an arrangement would result if a layer of carbon atoms at the (00$\bar{1}$) surface were replaced by a layer of oxygen atoms. Molecular oxygen can be a predominant influence in spin–lattice relaxation in open structures such as zeolites,[40] and presumably on surfaces as well, so this would provide a mechanism for efficient spin–lattice relaxation in a surface oxide layer. Correspondingly, the peaks at −44, −49, and −56 ppm might arise from tetrahedral silicon bonded to one oxygen and three carbons, the result of oxidation at the (001) surface. These shifts are consistent with the known wide ranges for $RSi(OR)_3$ and R_3SiOR,[41] but a number of other possible species would absorb in these regions too and cannot at present be excluded.[42] The peak observed at −78 or −79 ppm in a few samples is near the position of elemental silicon (−80.6 ppm[43]).

The broad underlying resonance, seen in both ^{29}Si and ^{13}C rapid-pulsing spectra of industrial samples, is reminiscent of the amorphous silicon carbide resonance but shifted from this position in a direction consistent with some oxygen incorporation, i.e., to

(31) Abragam, A. *The Principles of Nuclear Magnetism*; Clarendon: Oxford, 1961; Chapters V, IX. Abragam, A.; Goldman, M. *Nuclear Magnetism: Order and Disorder*; Clarendon: Oxford, 1982; Chapter VI.
(32) Maiti, B.; McGarvey, B. R. *J. Magn. Reson.* **1984**, *58*, 37.
(33) Iwamiya, J. H.; Gerstein, B. C. *Zeolites* **1986**, *6*, 181 and references therein.
(34) Axelson, D. E. *Solid State Nuclear Magnetic Resonance of Fossil Fuels: An Experimental Approach*; Multiscience Publications Limited: Canadian Government Publishing Centre, Supply and Services Canada, Ottawa, Ontario, Canada, 1985.
(35) Hageman, E. W.; Chambers, R. R., Jr.; Woody, M. C. *Anal. Chem.* **1986**, *58*, 387.
(36) Bloembergen, N. *Physica (Amsterdam)* **1954**, *20*, 1130.
(37) Hardeman, G. E. G. *J. Phys. Chem. Solids* **1963**, *24*, 1223. Alexander, M. N. *Phys. Rev.* **1968**, *172*, 331. Also see ref 4, pp 174–175.
(38) Maciel, G. E.; Sindorf, D. W. *J. Am. Chem. Soc.* **1980**, *102*, 7606. Coleman, B. In *NMR of Newly Accessible Nuclei*; Laszlo, P., Ed.; Academic: New York, 1983; Vol. 2, pp 197–228.
(39) Smith, J. V.; Blackwell, C. S. *Nature (London)* **1983**, *303*, 223.
(40) Cookson, D. J.; Smith, B. E. *J. Magn. Reson.* **1985**, *63*, 217. Klinowski, J.; Carpenter, T. A.; Thomas, J. M. *J. Chem. Soc. Chem. Commun.* **1986**, 956.
(41) Marsmann, H. In *NMR Basic Principles and Progress*; Diehl, P., Fluck, E., Kosfeld, R., Eds.; Springer-Verlag: Berlin, 1981; Vol. 17, pp 65–235.
(42) The silicon nitride chemical shift (α – Si_3N_4, −48.0 and −49.7 ppm; β – Si_3N_4, −48.5 ppm[18]) does correspond to one of our peaks, but silicon surrounded by four nitrogens seems implausible. Silicon surrounded by both nitrogen and oxygen is possible, however,[18] and a SiO_3N species might have a chemical shift near −97 ppm.
(43) Our MAS value; the literature value (nonspinning) is −85 ppm: Holzman, G. R.; Lauterbur, P. C.; Anderson, J. H.; Koth, W. *J. Chem. Phys.* **1956**, *25*, 172.

high field in the ^{29}Si spectrum and to low field in the ^{13}C spectrum.

The −32.4 ppm ^{29}Si peak, which becomes comparable in size to the three "crystalline" 6H peaks in some samples under very rapid pulsing (Figure 5d), is intriguingly close in chemical shift to the −31 ppm position that we proposed in section II as the probable chemical shift of type D silicon. Under rapid pulsing the bulk crystalline silicon carbide may not be contributing appreciably to the signal, and local crystalline regions with short T_1's, which need not be similar to the predominant polytype in the crystal, could provide most of the residual "crystalline SiC" contribution to the signal. Such anomalous short T_1 crystalline regions could well contain a range of polytypes, and a type D site might appear in spectra that discriminate in favor of nonstandard environments.

Hydrofluoric acid washing experiments were carried out to investigate the possibility that the short T_1 species are surface material. Oxide layers on silicon carbide crystal surfaces can be removed by treatment with aqueous hydrofluoric acid, which attacks Si–O bonds but leaves Si–C bonds unaffected.[44] Disappearance of most of the impurity ^{29}Si signals on HF washing of one sample does indicate that surface oxide material gives rise to much of the short T_1 signal intensity (Figure 7); however, spectra of other, apparently similar samples are almost unaffected by HF washing, suggesting that the material observed is in the interior; alternatively it might be passivated to HF. Further work is in progress.

V. **Amorphous Silicon Carbide.** The broadness of the ^{29}Si and ^{13}C resonances of amorphous silicon carbide (Figure 2) is consistent with a wide range of local environments and is reminiscent of ^{29}Si MAS NMR spectra of silicate glasses.[17] Peak maxima are in the same chemical shift range as crystalline silicon carbide polytypes, consistent with the typical silicon (and carbon) environments being not much different from those in the crystalline forms. Nicalon ceramic fiber is believed to be primarily microcrystalline β-SiC; we can obtain a ^{13}C spectrum from it, yet we have been unable to obtain a ^{13}C spectrum from good crystals of β-SiC (the 3C polytype). Further broadening of the ^{13}C signal of Nicalon fiber under rapid pulsing indicates that carbons with chemical shifts in the usual silicon carbide range, near the peak maximum, have longer T_1's and become saturated more readily, compared to the carbons in unusual environments which absorb outside this range. Shorter T_1's in the unusual environments could arise from greater atomic motion or alternatively from a greater concentration of paramagnetic impurities and are not inconsistent with the apparent extremely long T_1's of carbon atoms in well-crystalline β-SiC environments.

Summary

Our local-site designation system explains the number and relative intensities of ^{29}Si peaks of the 6H and 15R polytypes of silicon carbide and illuminates the intriguing mirror-image relationship between ^{29}Si and ^{13}C spectra. Questions remain concerning the ^{13}C spectrum of the 15R polytype. Unavailability of additional polytypes has limited this work. While large crystals of some polytypes have been reported, many of the known but uncommon polytypes have been prepared only as very small single crystals or as syntactically coalesced twins with other polytypes and thus are unsuitable for NMR study. The formation of a particular polytype is a hit-or-miss process, and powder-pattern or single-crystal X-ray diffraction is necessary to identify each individual crystal. The 2H polytype would be of particular interest as it contains the rare type D site, which should have unique ^{29}Si and ^{13}C chemical shifts. Spectra of additional polytypes should confirm that types A–C chemical shifts are very similar in all α-SiC polytypes. The analysis presented here is applicable to all polytypes of silicon carbide and will provide a focus for further work. As a direct probe of the nuclear environment, MAS NMR should complement the many other physical methods that have been applied to silicon carbide. Many different aspects of NMR, including potential applications to high-tech ceramics and study of minor impurity species, come together in the NMR study of silicon carbide, making this a fruitful field for further research. Polytypism provides an excellent opportunity to systematically study the effects of lattice site on chemical shift, and studies of other polytypic systems are in progress with this goal in mind.

Acknowledgment. We are deeply indebted to the late Dr. G. R. Finlay for providing the samples that initiated this work and for helpful discussions. We thank the Natural Sciences and Engineering Research Council of Canada for financial support, the Ministry of Colleges and Universities, Province of Ontario, for the award of an Ontario Graduate Scholarship (to B.G.W.), Prof. C. A. Fyfe, Dr. R. E. Lenkinski, Dr. E. C. Kelusky, and Mr. W. Klimstra for assistance with the instrumentation, and Mr. K. Nair and Dr. L. Wolfe of General Abrasive, Niagara Falls, for providing the industrial production-run samples and for helpful discussions. Further samples were provided by Dr. R. Van de Merwe of the Norton Co., Dr. C. Schilling of Union Carbide, Dr. P. E. D. Morgan of Rockwell International, and Prof. D. R. Peacor of the University of Michigan. We also thank Mr. P. Brown for drafting, Mr. J. Elman of Eastman Kodak for obtaining ESCA spectra, and Mr. A. G. Basile and Mr. R. Routhier for technical assistance. The NMR spectra were obtained at the South Western Ontario High Field NMR Centre, funded by a Major Installation Grant from NSERC.

Note Added in Proof. Chemical shift calculations carried out since this paper was submitted show that magnetic anisotropy effects from distant bonds can account for the relative peak positions observed. The mirror-image relationship observed in the 6H polytype ^{29}Si and ^{13}C spectra is apparently a coincidence, with type A atoms absorbing at lowest field in both sets of spectra. Distant neighbors affect chemical shifts to a sufficient extent that more than three ^{13}C peaks are predicted for the 15R polytype, as observed. Details of the calculations will be published separately.

Registry No. SiC, 409-21-2.

(44) Brynestad, J.; Bamberger, C. E.; Heatherly, D. E.; Land, J. F. *J. Am. Ceram. Soc.* **1984**, *67*, C-184.